

Optimum Design of Conformal Array Antenna with a Shaped Radiation Pattern and Wideband Feeding Network

M. H. Rahmani and A. Pirhadi

Department of Electrical Engineering
Shahid Beheshti University G.C (SBU), Tehran, Iran
mohammadhassan.rahmani.1@ens.etsmtl.ca, a_pirhadi@sbu.ac.ir

Abstract— In the present work, a circular conformal array with wideband printed dipole antennas and wideband feeding network has been designed to obtain a fully constrained cosecant squared radiation pattern using particle swarm optimization (PSO) algorithm and mutual coupling compensation. Using the circular conformal design leads to a decrease of around 33% of the length of the array antenna compared with that of the vertical linear array. Moreover, a better performance of the coverage region and side lobe fall after this area obtains by using this configuration.

Index Terms - Conformal array antenna, mutual coupling, particle swarm optimization, shaped beam, and wideband feeding network.

I. INTRODUCTION

Conformal antennas were first introduced in avionics to be integrated with the curve shape of the aircrafts in order to overcome aerodynamic limitations. Nowadays, in order to decrease the physical size of the array antenna or fit it with different shapes, conformal arrays are widely used in various vehicles, high speed trains, satellites, and military surveillance radars. The implementation of some radiation patterns is more accessible using the conformal arrays and they can overcome both physical and radiation patterns restrictions. Different microstrip conformal arrays have been introduced in the literature [1-3]. Shaped beam array antennas are of a great interest in the wireless community. The key aspect in the design of this type of array antennas is to set the elements excitations including phase and amplitude and the position of array elements to obtain a desired radiation pattern. To this end different analytical and numerical methods have been proposed until now [4]. However, in recent years, with the

emergence of evolutionary optimization methods like genetic algorithms, differential evolution, and particle swarm optimization lots of researches have been carried out for the design of array antennas [5-7]. The design and synthesis of an array antenna for a desired radiation pattern is often affected by the mutual coupling effect between its elements. In fact, this effect will cause in a difference between the theoretical synthesis and the practical implementation [8]. In order to consider the far field mutual coupling of the elements in the synthesis process, the complex active radiation pattern of each element in the presence of the other elements must be used [9-11]. The particle swarm optimization (PSO) is a well-known evolutionary search method that has been used in different electromagnetic applications including array antennas throughout the last decade. In contrast with other stochastic algorithms, the PSO is proven to be easier to implement, adjust, and realize. Moreover, with a good choice of the initial values, the PSO can be guided in order to reach a more applicable result with a better timing efficiency [12-16].

In this paper, a new method of synthesis and design of the conformal array antenna has been proposed. Because of the variation of elements orientation and mutual coupling effect, the radiated fields of elements are different from each other and it must be considered in the array factor equation, which is used by the PSO. Independent from the shape of the conformal array, this method can be developed for the design of various shapes of the conformal array in which only the active complex patterns of each elements vary in the array factor. This method is fast, easy to implement, and avoids complicated calculations. The conformal array, which is synthesized and designed in this research is a circular array for surveillance

radars applications.

The feeding network has an important role in the array antenna design because the resulting radiation pattern and bandwidth of the whole system is highly dependent on it. Various methods have been used to design and implement the feeding network [1]. However, for a shaped radiation pattern, the feeding network design includes more challenges as it includes various phase shifters and power dividers. The usage of Wilkinson power dividers and delay line phase shifters has the advantage of delivering the exact decimal powers and phase shifts. However, they suffer from isolation issues and highly dependency with the frequency [29]. In this paper, we use a novel approach to design a feeding network that can deliver non-symmetric accurate powers and phase shifts with Wilkinson power dividers and wideband delay line phase shifters in the whole desired frequency band. The structure of this article is as follows: section II consists of an introduction to the development of the PSO for current project. In section III, the element that is used in the array and the conformal array configuration are presented and detailed. Section IV presents the simulation results with an investigation in mutual coupling compensation using complex active element patterns and the PSO. The fifth section is dedicated to the design of the wideband feeding network, which provides a stable phase shift and power splitting over the whole bandwidth.

II. USING THE PSO TO SYNTHESIZE OF CONFORMAL ARRAY ANTENNA

Generally, the parameters to control the radiation pattern of an array antenna are the amplitude and phase of excitation current of array elements [1]. The far-field array factor for a linear phased array of isotropic elements with inter-element distance of d and the wave number of $k = 2\pi d/\lambda$, which is placed on the z -axis, is $AF(\theta) = \sum_{n=1}^N A_n e^{jkn \cos \theta + j\varphi_n}$, where λ is the free space wavelength, n is the element number. A_n and φ_n are the amplitude and phase excitation of the n^{th} element, respectively. The goal is to define these amplitudes and phases using the PSO algorithm. Because of the mutual coupling effect and the changing the elements' direction in the conformal array, the active pattern of each element is different from the other elements. For this matter we have to consider the amplitude and phase of the pattern of each element in the

presence of other elements, which is named, $E_n(\theta, \varphi)$ where θ and φ are the angular coordinates of a point in far field. In the following simulations θ changes from 0° to 180° while φ is 0° and -180° . The radiation pattern equation [7-8] is,

$$F(\theta, \varphi) = \sum_{n=1}^N A_n e^{j\varphi_n} E_n(\theta, \varphi). \quad (1)$$

A_n and φ_n represent the amplitude phase of the n^{th} element excitation, respectively. In the above formulation the information related to the positioning of the elements is stored in $E_n(\theta, \varphi)$.

In 1995, Eberhart and Kenedy introduced the particle swarm optimization algorithm, which was an imitation of swarms of fish, bees, and birds when exploring the space to find the maximum amount of food. The importance of this algorithm is due to its fast and precise convergence, simple calculation steps, and easy implementation, which are the result of the Newtonian law of motion, which is the foundation of this algorithm [17-18]. The PSO is used to optimize continuous and discrete functions and is widely used in electromagnetic. It has been implemented in different applications like pattern synthesis of array antennas, reflector antennas optimization, corrugated horns optimization, patch antennas design, frequency selective surfaces, and microwave absorbers [19-22]. Tedious works in the field of array antenna synthesis using the PSO have been carried out until now [11-15, 19-24]. In the following section the PSO is developed for conformal array optimization.

A. Development of the PSO

In the original PSO, particles (amplitude and phase of the elements) are generated randomly and they can displace freely within the imposed boundary values of the solution space [17]. Although this will reduce the probability of immature convergence and increases the preciseness of the method, it usually leads to non-realistic amplitudes and phases and sometimes makes the implementation of the feeding network impossible. If the relative amplitude of two adjacent elements is too much, the fabrication of the related power splitter will be practically impossible as it will need too thick arms. Moreover, in the point of view of phases, high inter-element phase difference will make the construction of the wideband phase shifters more difficult.

The original PSO algorithm is developed to control massive changes of inter-elements amplitudes and phases of the excitations. To this end, the domain of input random variables is divided between elements to control the relative amplitudes and phase differences between adjacent elements. This means that X_1 is no longer a matrix of a completely random numbers between X_{\max} and X_{\min} , but it is guided in such a way that each number is allowed to be chosen randomly in restricted domain, which is defined as follows,

$$s = \frac{x_{\max} - x_{\min}}{n} \quad (2)$$

$$a(\mu_n) = X_{\min} + (\mu_n - 1)s, \quad (3)$$

$$X = \{a(\mu_n) + (a(\mu_n + 1) - a(\mu_n))\gamma\}. \quad (4)$$

In the above formulation $\mu_n = \{1, 2, \dots, N\}$ according to the n^{th} element of the array, and γ is a random number between $[0, 1]$. X_{\max} and X_{\min} are, respectively the maximum and the minimum of acceptable values for amplitudes and phases. Then, the position of the particles through the algorithm is updated using equations (5) and (6),

$$V_{k+1}^i = w_k V_k^i + r_1 c_1 (Pb^i - X_k) + r_2 c_2 (Gb - X_k) \quad (5)$$

$$X_{k+1}^i = X_k^i + V_{k+1}^i, \quad (6)$$

where V_k^i is the velocity of the i^{th} particle in the k^{th} iteration, X_k^i is the position of the i^{th} particle in the k^{th} iteration. w_k is the weighting coefficient of the k^{th} iteration, r_1 and r_2 are random matrices, and $c_1 = c_2 = 2$ are called the acceleration coefficients. Pb^i is the best position of the particle i^{th} during its exploration and Gb is the global best of the whole group. The weighting coefficient, w , is set to change linearly with equation (7),

$$w_k = w_{\max} - \frac{(w_{\max} - w_{\min}) * (k-1)}{k_{\max}}, \quad (7)$$

where k is the iteration number with the maximum of $k_{\max} = 150$, $w_{\min} = 0.2$ is the minimum of the weighting factor, and $w_{\max} = 0.9$ is its maximum. As a result of applying such procedure for obtaining the initial values, the relative amplitude and inter-element phase difference is controlled and massive changes, which lead to the complexity of the feeding network are avoided. In order to increase the efficiency of the algorithm the desired pattern is divided to different parts and the error for each part is calculated with different weights. As shown in Fig. 1, the desired pattern is a cosecant squared pattern, which is divided into 4 regions

with different weights.

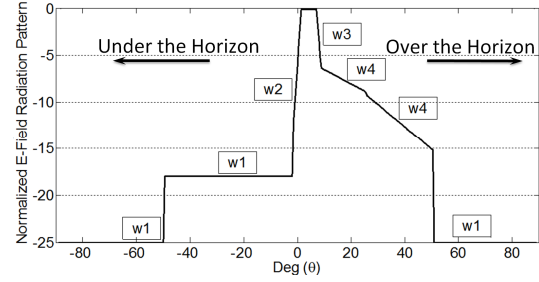


Fig. 1. Desired pattern with different weighting parts.

The error for this desired pattern is calculated as presented in equation (8),

$$\begin{aligned} Error = & w1 \sum_{-90}^{a1} |F_d - F_N| + w2 \sum_{a1+1}^{a1-1} |F_d - F_N| + \\ & w3 \sum_a^b |F_d - F_N| + w4 \sum_{b+1}^{b1} |F_d - F_N| + \\ & w4 \sum_{b1+1}^{90} |F_d - F_N| \end{aligned} \quad (8)$$

where F_d is the desired pattern and F_N is the normalized calculated array factor, which is given in each iteration using the amplitudes and phases delivered by the algorithm. $w1$, $w2$, $w3$, and $w4$ are the weights. In the above illustration, the region between 0° and 50° is called the coverage region of the radiation pattern, and consequently, 50° to 60° is the quick fall region and 60° to 90° is the side lobe region. Aside from the physical length of the array antenna, another advantage of using the conformal shape of the array is that it can deliver a better performance in the coverage and quick fall regions, which will be shown in next sections. This shape has been used in military surveillance radars and includes various imposed constraints such as different side lobe levels and horizon angles.

III. ANTENNA ARRAY CONFIGURATION

A. Wideband microstrip dipole antenna

The designed array consists of 8 elements of wideband microstrip dipole array (MDA) with balun working at the centre frequency of 1.1 GHz. It has been generally proved that MDA needs a balanced feed that could be a $\lambda/4$ coaxial balun. For a printed dipole this could be replaced by an integrated balun, which delivers broadband performance [25] and has been used in antenna array applications [26]. To achieve a better impedance matching with 50Ω with wideband performance, instead of using a

quarter wavelength transformers, the feed point of the integrated balun is adjusted as described in [27]. The schematic of the single element reflection coefficient of the MDA is shown in Fig. 2 (a). Also the normalized E-field radiation amplitude and phase of this antenna are depicted in Fig. 2 (b) and (c).

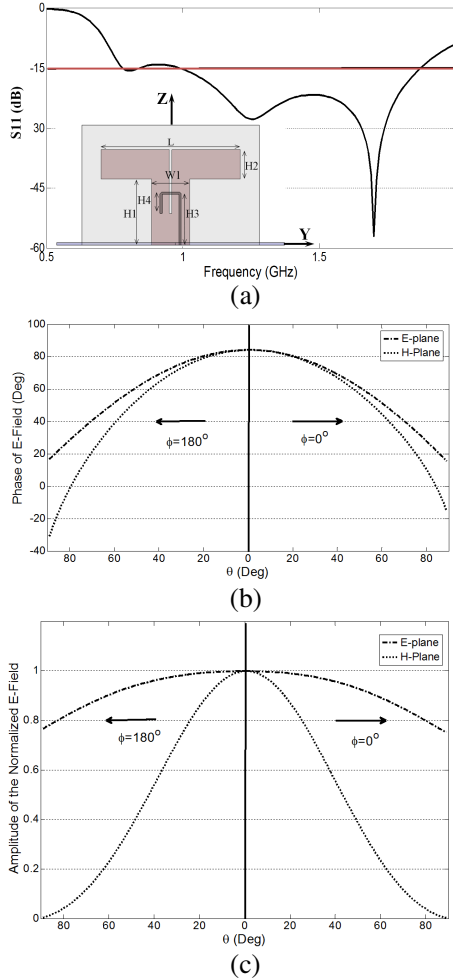


Fig. 2. Single printed dipole antenna with $H1 = 52$ mm, $H2 = 23$ mm, $H3 = 40$ mm, $H4 = 15.3$ mm, $l = 30$ mm, $L1 = 110$ mm: (a) reflection coefficient, (b) phase of radiated E-fields, and (c) amplitude of radiated E-fields.

B. Conformal array configuration

In this section, three different array configurations are presented, simulated, and synthesised to derive the desired radiation pattern. The first configuration is a linear array of 8 MDA elements. The schematic view of the array is shown in Fig. 3 (a). As it is seen it has a height of 1200 mm. In order to decrease the height and obtain a low profile configuration,

another configuration (Fig. 3 (b)), which consists of a diagonal array with an angle of 45° related to the horizontal plane is presented. The height of this configuration is 860 mm, which is 28.3 % smaller than the vertical configuration. However, to obtain a smaller array the third array structure, which is a circular conformal array is presented that has a height of 800 mm, thus providing a physical size of around 33 % smaller than the first linear structure. For this array the MDA elements are implemented on the outer surface of a sphere with the radius of 800 mm. Figure 3 (c) depicts the circular array antenna. The inter-element distance for these three arrays is 0.8λ at the centre frequency of 1.1 GHz.

The antennas are printed on an Ro4003 substrate with a relative dielectric constant of $\epsilon_r = 3.38$ and a thickness of 32 mil. Moreover, a ground plane is designed in the array structure in order to increase the array directivity. The simulation and analysis has been performed by Ansoft HFSS [30] software based on the finite element method.

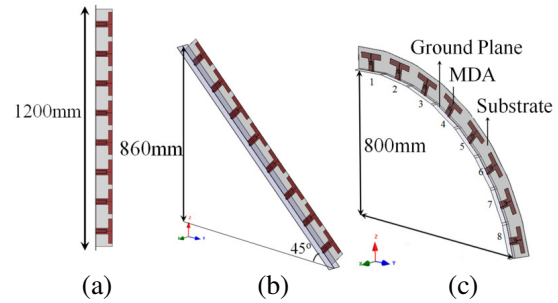


Fig. 3. Array configurations, (a) the linear array, (b) the diagonal array, and (c) the circular conformal array.

IV. OPTIMIZATION AND SIMULATION PROCEDURE

A. Array synthesis with an investigation of the array structure

As mentioned in the previous section, due to the presence of mutual coupling between the array elements, the radiation patterns of the array elements are different from each other. Therefore, we have to use the complex active radiation fields to calculate the radiation pattern of the array. The active radiation patterns of some elements of the conformal circular array are shown in the Fig. 4 (a) and (b) as terms of amplitude and phase. It is clearly observed that the far-field pattern of each element is different from that of others.

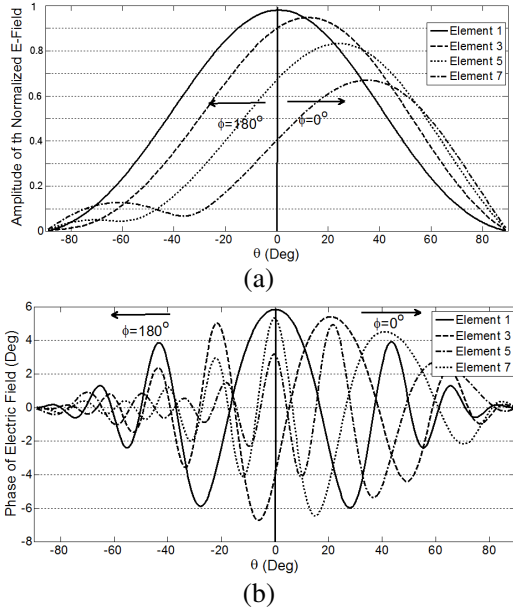


Fig. 4. (a) The normalized E-fields of elements 1, 3, 5, and 7 in the array and (b) the phase of E-field of elements 1, 3, 5, and 7 in the array.

B. Simulation and optimization results

First, using the three mentioned array structures in Fig. 3, we have performed the PSO in Matlab to synthesize a cosecant squared radiation pattern with a coverage region of 50°. Figure 5 (a) represents the convergence rate of the applied developed PSO and Fig. 5 (b) depicts the resulted radiations patterns.

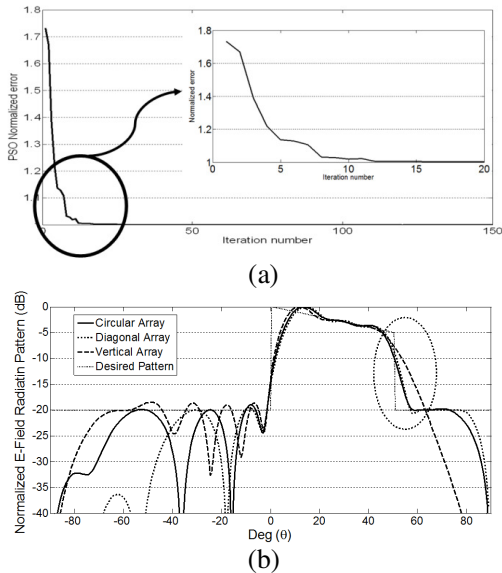


Fig. 5. (a) Convergence diagram of the PSO and (b) optimized E-field radiation pattern of three array antennas for coverage area of 50°.

The algorithm converges in less than 50 iterations. As it is seen in Fig. 5 (b), all these three arrays can produce the desired coverage, however, the circular and the diagonal arrays have a better performance right after 50°. In other situation, for wider coverage region, the desired radiation pattern has been changed in such a way to produce a coverage region of 60°. We have performed the PSO method to synthesize and compare the resulting radiation patterns of these three arrays. The result has been shown in Fig. 6.

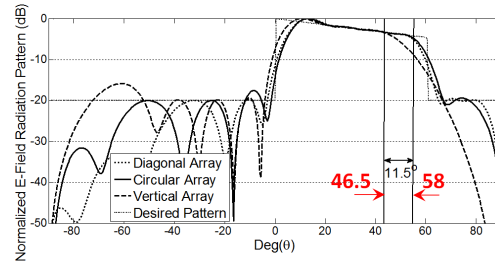


Fig. 6. Optimization resulted E-field radiation pattern of three arrays for coverage area of 60°.

As it is observed in Fig. 6, the diagonal and the circular array can produce the wider coverage region with respect to linear array. As a result, we conclude that the circular conformal array is more advantageous than the diagonal and the linear array because:

- 1- It has a smaller physical height than the diagonal and the linear array.
- 2- It has a better side lobe level fall than the linear array.
- 3- Its resulted coverage region is wider than the linear array.

C. Simulation of the final synthesized array

As was mentioned, the conformal circular array can produce the wider coverage region and better side lobe level fall with smaller physical height. Hence, this structure has been used in the following section to synthesize the desired radiation pattern of Fig. 1. In order to show that the mutual coupling effects on the radiation pattern have been fully considered and compensated, the resulted amplitudes and phases from the PSO process have been used as the element excitations of the simulated array in the Ansoft HFSS software. The resulted E-field radiation patterns from the PSO and the simulation have been compared in Fig. 7. As it is seen, these two radiation patterns have good agreement because the mutual coupling is fully

considered in the optimization process. The derived amplitudes and phases are shown in Fig. 8. It is seen that, by using the developed PSO method, the relative amplitude between the adjacent elements are between 0.5 and 1. Moreover, the phase differences between the adjacent elements are between 0° and 150° . These ease the complexity of making the feeding network.

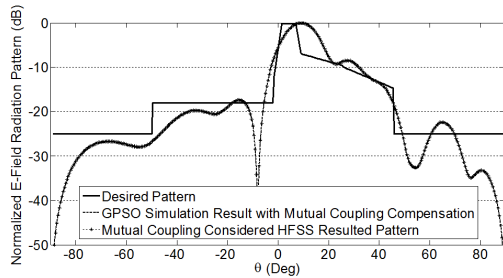


Fig. 7. Radiation pattern of normalized E-field of 8 elements MDA with far field mutual coupling compensation.

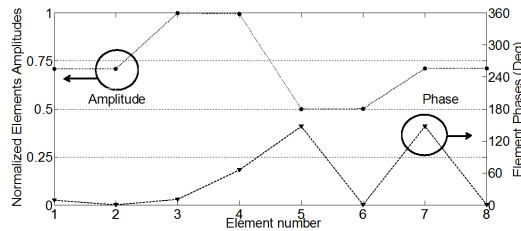


Fig. 8. Amplitudes and phases excitation of the array.

V. DESIGN OF THE FEEDING STRUCTURE

After determining the optimum amplitudes and phases of the array elements, to obtain the desired radiation pattern, it is necessary to design a suitable feeding network. In this case, as a result of using the developed PSO, the inter-element phase shift is linear and limited so that the phase shifters are easier to design. Moreover, the inter element relative amplitudes are limited and easily possible to implement.

The feeding network consists of some non-symmetrical and symmetrical power dividers. The optimum tapering of amplitudes of the array elements is obtained by adjusting the ratio of power dividers. As mentioned before, embedded active element patterns combined with the PSO are used to compensate the far-field mutual coupling. However, the inter-port coupling is an important issue that affects greatly the performance of the designed array. To minimize

this effect, the Wilkinson power dividers that provide two isolated ports are used to isolate the output ports and minimize the inter-port coupling [28]. In addition, to obtain the optimum phase distribution in the operating frequency, the delay line phase shifters are used to adjust the phases of the elements. The most challenge in the design of the feeding network is the narrowband behaviour of the delay line phase shifters. For this application, the desired bandwidth is about 30% in the centre frequency of 1.1 GHz and it requires designing the wideband phase shifters.

A. Designing the feed network at the centre frequency

The schematic view of the feeding network before phase shift correction is shown in Fig. 9.

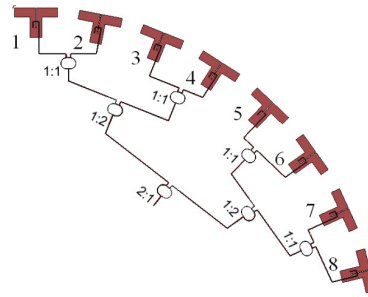


Fig. 9. Schematic view of the feeding network before phase shift correction.

In Fig. 9 the values of the power dividers are described based on the splitting ratio of each arm. For example, 1:2 means that the right arm takes twice the power than the left arm. Each power divider has its own power splitting ratio based on the optimization results.

To design the feed network, at first, each equal and non-equal Wilkinson power divider is separately designed according to the desired power splitting ratio and desired phase shift at the centre frequency. The dimensions of the Wilkinson power dividers that have been used in this feeding network have been shown in Fig. 10. Then the whole feed network is made by uniting these separate power dividers. At this step, the feeding network delivers the proper power to each element with the desired phase shift at the centre frequency. The simulation of the power dividers, phase shifters, and the whole feeding network has been done in HFSS software. The output powers of this feeding network over the desired frequency band are shown in Fig. 11.

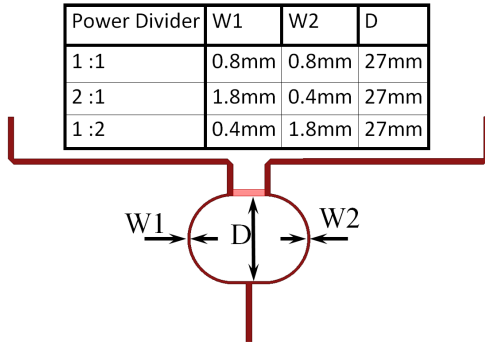


Fig. 10. Wilkinson power divider dimensions.

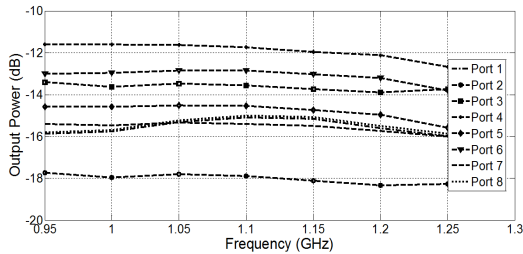


Fig. 11. Resulted output power of each port.

The results show that the output power produced by each port is nearly stable over the whole frequency band and does not need correction. Figure 12 shows the resulted phase shift of each port.

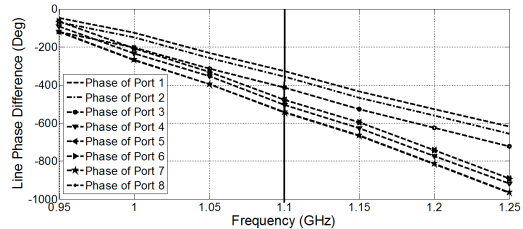


Fig. 12. Resulted output phase shift of each port.

As it is seen in Fig. 12, due to the different lengths of paths, the phase difference between the ports are not stable over the whole frequency band and the slope of the phase shifts is different for each output port. This will result in the degradation of the resulted pattern thus making the need for phase shift correction indispensable.

B. Output phase difference correction within the desired bandwidth

To correct the resulted phase differences in such a way that they become stable over the whole frequency band the following steps should be performed. First, we have to find the port

with the maximum slope and consider it as reference. Here the reference port is port No. 8 as it has the longest length. Then, by increasing the length of the microstrip lines in other routes and also using wideband phase shifters we have to increase the phase slope of other ports to reach the reference slope. All this procedure should be executed in such a way that the phase shift does not change at the center frequency. The wideband phase shifter consists of a wilds phase shifter, which is fully described in [29]. It consists of two open and short circuited $\lambda/8$ stubs or one $\lambda/4$ circuited open stub. By changing the ratio of $W1/W2$ it is possible to obtain different phase shifts with increasing the slope of the phase shift of the line. Figure 12 shows the phase shift slope correction of the above phase shifters. Table 1 summarizes the wideband phase shifters that are used in this paper along with their dimensions.

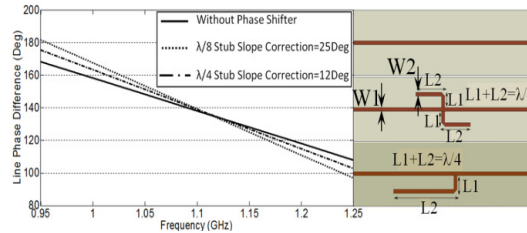


Fig. 13. Wilds phase shifters and their phase difference corrections.

Table 1: Wideband wilds phase shifters used in this project with their dimensions.

	W1/W2	Resulted Phase Shift
Double Stub	18	54°
Double Stub	3	25°
Double Stub	0.36	150°
Single Stub	1	33°

C. Final wideband feeding network

By executing the previously described phase shift correction procedure, a wideband feeding network with stable phase shift and power split ratio is achieved. The schematic view of the final feeding network is shown in Fig. 13. Figure 15 shows the resulted output phase shifts after the phase correction procedure over the whole frequency band.

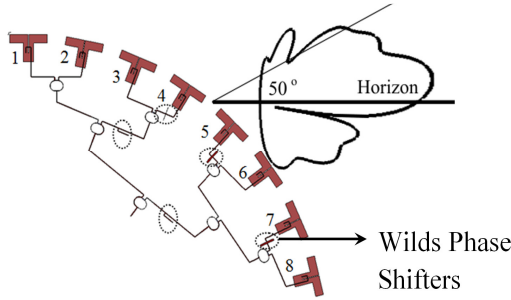


Fig. 14. Final feeding network and array antenna structure after phase shift correction.

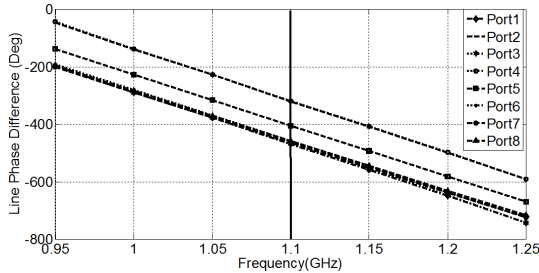


Fig. 15. Output phase shift of each port after correction.

As seen in this figure, after the phase shift correction procedure, the slope of the output phase shift for all ports is finally equal, and consequently, the phase difference between ports is stable within the whole frequency band. Figure 16 shows the output power of the final feeding network.

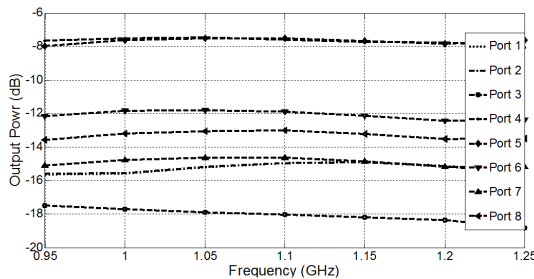
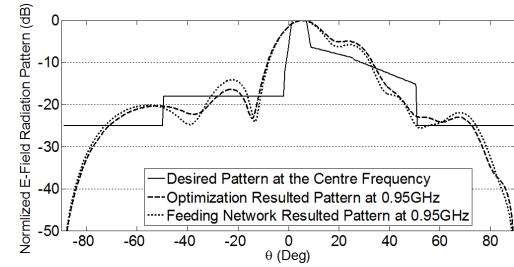


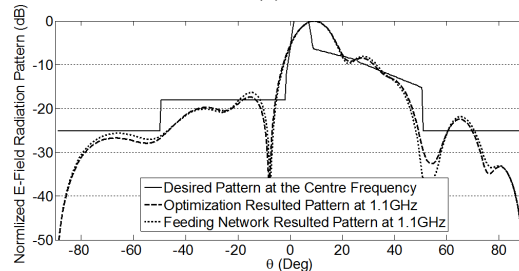
Fig. 16. Output power of each port after correction.

The resulted output power is almost stable in desired bandwidth and no correction is needed for this case. To finalize the design of the MDA array, the designed array and the wideband feeding network are united and simulated all together. The final results are shown in Fig. 17. In this figure, the resulted radiation pattern of the optimization algorithm, which had been

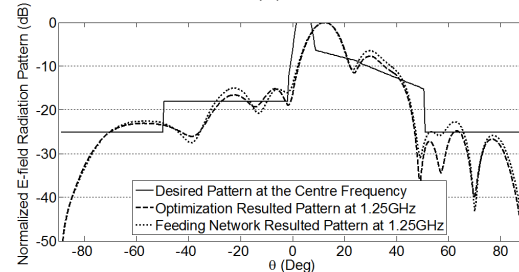
performed in the center frequency has been compared with the feeding network output results at 0.95 GHz, 1.1 GHz, and 1.25 GHz. It is well depicted that the resulted patterns by the feeding network have good agreement with that of the optimization results of the center and the end of the desired frequency band.



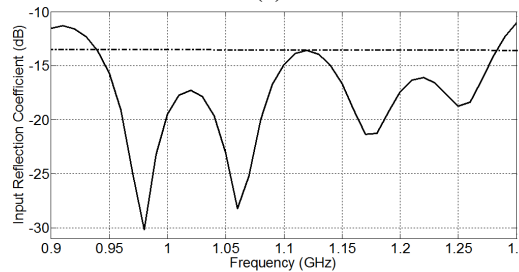
(a)



(b)



(c)



(d)

Fig. 17. Final E-field radiation pattern (a) $f = 0.95$ GHz, (b) $f = 1.1$ GHz, (c) $f = 1.25$ GHz, and (d) the input reflection coefficient of the array antenna.

VI. CONCLUSION

In this article, a circular conformal array has been designed, analyzed and simulated to obtain

a fully constrained cosecant squared pattern using a modified PSO algorithm. The designed array consists of an 8 elements printed dipole with the inter-element distance of $d = 0.8 \lambda$ working at the central frequency of 1.1 GHz and placed on the outer surface of a sphere with the radius of 800 mm. The comparison between a vertical linear array, diagonal linear array and the circular conformal array with the same inter-element distance depicted that the height of the former array is 33% less than that of the vertical linear array and near 7% less than that of the diagonal array, thus producing a lower profile array antenna. Moreover, the performance of these three arrays on the coverage area and side lobe fall after this area has been investigated and it has been observed that the circular and the diagonal arrays have a quicker fall right after the coverage area and can produce a wider coverage region. The PSO algorithm, along with the method of the active element patterns has been used to synthesize the array with the consideration of the far field mutual coupling. Finally, a wideband and isolated feeding network, which is able to produce desired excitations for a consistent cosecant squared pattern over the desired frequency band has been designed using equal and non-equal Wilkinson power splitters and wideband phase shifters.

REFERENCES

- [1] L. Josefsson and P. Persson, *Conformal Array Antenna Theory and Design*, USA: John Wiley and Sons, 2006.
- [2] A. Zaghoul, M. Parsa, and S. Kumar, "Investigation of a microstrip antenna array conformal to a paraboloidal surface," *23rd Annual Review of Progress in Applied Computational Electromagnetics (ACES)*, pp. 1608-1615, Italy, March 2007.
- [3] K. Xiao, Y. Li, F. Zhao, S. Chai, and J. Mao, "Analysis of microstrip antennas using the volume surface integral equation formulation and the pre-corrected fast Fourier transform method," *Applied Computational Electromagnetics Society (ACES) Journal*, vol. 26, no. 11, pp. 922-929, Nov. 2011.
- [4] D. Kurup, M. Himdi, and A. Rydberg, "Synthesis of uniform amplitude unequally spaced antenna arrays using the deferential algorithm," *IEEE Trans. Antennas Propagat.*, vol. 51, pp. 2210-2217, 2003.
- [5] D. Gies and Y. Rahmat-Samii, "Particle swarm optimization for reconfigurable phase differentiated array design," *Microwave and Optical Technology Letters*, vol. 38, no. 3, 2003.
- [6] D. W. Boeringer and D. H. Werner, "Particle swarm optimization versus genetic algorithms for phased array synthesis," *IEEE Trans. Antennas Propagat.*, vol. 52, no. 3, 2004.
- [7] I. Gupta and A. Ksienski, "Effect of mutual coupling on the performance of adaptive arrays," *IEEE Trans. Antennas and Propagat.*, vol. 31, no. 5, pp. 785-791, 1983.
- [8] D. Kelley and W. Stutzman, "Array antenna pattern modelling method that includes mutual coupling effects," *IEEE Trans. Antennas Propagat.*, vol. 41, pp. 1625-1632, 1993.
- [9] P. Darwood, P. Fletcher, and G. Hilton, "Mutual coupling compensation in small planar array antennas," *IEE Proc. Microw. Antennas Propagat.*, vol. 145, pp. 1-6, 1998.
- [10] P. Fletcher and M. Dean, "Derivation of orthogonal beams and their application to beamforming in small phased arrays," *IEE Proc. Microw. Antennas Propagat.*, vol. 143, pp. 304-308, 1996.
- [11] S. Zhang, S.-X. Gong, Y. Guan, and S. Zhang, "A novel IGA- PSO hybrid algorithm for the synthesis of sparse arrays," *Progress in Electromagnetics Research*, vol. 89, pp. 121-134, 2009.
- [12] Z. Hang, S.-X. Gong, and S. Zhang, "A modified PSO for low sidelobe concentric ring arrays synthesis with multiple constraints," *Journal of Electromagnetic Waves and Applications*, vol. 23, no. 11, pp. 1535-1544, 2009.
- [13] J. Pérez and J. Basterrechea, "Hybrid particle swarm-based algorithms and their application to linear array synthesis," *Progress in Electromagnetics Research*, vol. 90, pp. 63-74, 2009.
- [14] Z. Zaharis, S. Goudos, and T. Yioultis, "Application of boolean PSO with adaptive velocity mutation to the design of optimal linear antenna arrays excited by uniform amplitude current distribution," *Journal of Electromagnetic Waves and Applications*, vol. 25, no. 10, pp. 1422-1436, 2011.
- [15] M. Rahmani and A. Pirhadi, "Shaped beam microstrip dipole antenna synthesis using guided particle swarm optimization," *ACES Conference*, 2012.
- [16] S. Walker and D. Chatterjee, "Study of exact and high-frequency code solvers for applications to a conformal dipole array," *Applied Computational Electromagnetics Society (ACES) Journal*, vol. 24, no. 6, pp. 550-558, Dec. 2009.
- [17] J. Kennedy and R. Eberhart, "Particle swarm optimization," *Proc. IEEE Int. Conf. Neural Networks*, vol. 4, pp. 1942-1948, 1995.
- [18] R. Eberhart and Y. Shi, "Particle swarm optimization, developments, applications, and

- resources,” *Proc. Cong. Evol. Comput.*, vol. 1, pp. 81-86, 2001.
- [19] J. Robinson and Y. Rahmat-Samii, “Particle swarm optimization in electromagnetics,” *IEEE Trans. Antennas Propagat.*, vol. 52, no. 2, pp. 397-407, Feb. 2004.
- [20] D. Gies and Y. Rahmat-Samii, “Particle swarm optimization (PSO) for reflector antenna shaping,” *IEEE Antennas Propagat. Soc. Int. Symp. Dig.*, vol. 3, pp. 2289-2293, June 2004.
- [21] W. Liu, “Design of multiband CPW-fed monopole antenna using a particle swarm optimization approach,” *IEEE Trans. Antennas Propagat.*, vol. 53, no. 10, pp. 3273-3279, Oct. 2005.
- [22] S. Genovesi, R. Mittra, A. Monorchio, and G. Manara, “Particle swarm optimization for the design of frequency selective surfaces,” *IEEE Antennas Wireless Propagat. Lett.*, vol. 1, no. 5, pp. 277-279, Dec. 2006.
- [23] W. Li and X. Shi, “An improved particle swarm optimization algorithm for pattern synthesis of phased arrays,” *Progress in Electromagnetics Research*, PIER vol. 82, pp. 319-332, 2008.
- [24] S. Goudos, V. Moysiadou, T. Samaras, K. Siakavara, and J. Sahalos, “Application of a comprehensive learning particle swarm optimizer to unequally spaced linear array synthesis with sidelobe level suppression and null control,” *IEEE Antennas and Wirel. Propag. Lett.*, vol. 9, 2010.
- [25] B. Edward and D. Rees, “A broadband printed dipole with integrated balun,” *Microw. J.*, pp. 339-344, May 1987.
- [26] J.-P. Bayard, “Analysis of infinite arrays of microstrip-fed dipoles printed on protruding dielectric substrates and covered with a dielectric radome,” *IEEE Trans. Antennas Propagat.*, vol. 42, pp. 82-89, Jan. 1994.
- [27] R. LinLi, T. Wu, B. Pan, K. Lim, J. Laskar, and M. Tentzeris, “Equivalent circuit analysis of a broadband printed dipole with adjusted integrated balun and an array for base station applications,” *IEEE Trans. Antennas Propagat.*, vol. 57, no. 7, July 2009.
- [28] E. Wilkinson, “An N-way hybrid power divider,” *IRE Trans. on MTT*, vol. 116, Jan. 1960.
- [29] R. Wilds, “Try $\lambda/8$ stubs for fast fixed phase shifts,” *Microwaves and RF*, vol. 18, pp. 67-68, 1979.
- [30] <http://www.ansys.com/Products/Simulation+Technology/Electromagnetics/Signal+Integrity/ANSYS+HFSS>



Mohammad Hassan Rahmani received his B.Sc. and M.Sc. degrees in Electrical Engineering 2008 and 2011 from Azad University, Tehran, Iran and Shahid Beheshti University (SBU), Tehran, Iran, respectively. His major research interests are the development and design of wideband phased array antennas for wireless communications, evolutionary algorithms, and shaped beam antennas synthesis. He is currently pursuing his Ph.D. studies at École de Technologie Supérieure in Montreal, Canada.



Abbas Pirhadi received B.Sc. degree in Electrical Engineering from the Isfahan University of Technology, Isfahan, Iran 2000, and M.Sc. and Ph.D. degree in Communication Engineering from Tarbiat Modares University (TMU), Tehran, Iran in 2002 and 2007, respectively. From 2002 to 2006, he joined the antenna and propagation group of the Iran Telecommunication Research Center (ITRC) as a researcher. Also, in 2008 he joined the Shahid Beheshti University (SBU) where he is the Assistant Professor at the faculty of Electrical and Computer engineering. His research interests include microwave antennas, theoretical and computational electromagnetic with applications to antenna theory and design.